



Analysis of Mass Transfer During Natural Gas Purification Process in a Vertical Tube

Tansel KOYUN^{1,*}, Mehmet KUNDUZ¹, Hakan F. ÖZTOP²

¹*Department of Mechanical Engineering, Suleyman Demirel University, 32260 Isparta, Turkey*

²*Department of Mechanical Engineering, Technology Faculty, Firat University, TR-23119, Elazig, Turkey*

Received: 15/09/2012 Accepted: 10/12/2013

ABSTRACT

The effects of axial and radial velocities on mass transfer during the purification of natural gas in a vertical pipe are studied numerically. The natural gas flowing inside a vertical channel and monoethanolamine (MEA) flowing as a film along the inner wall of the channel is taken together for the purification process. The direction of laminar flow of both fluids is gravity direction. The environment is assumed as isothermal. Comparisons are performed for the interface (wall) between the film and the gas in the presence and absence of axial mass flow. Grams' finite difference formulation are used to solve governing equations and solved by using Grams' package code. It is found that the interface axial velocity effect on mass transfer can be neglected for low Reynolds numbers.

Keywords: Natural gas, Purification, Mass transfer, Reynolds number

Nomenclature

c	molar concentration, mol/cm ³
Da	Damköhler number
$D_{ij,B}$	polynary diffusion coefficient, cm ² /s
\bar{D}_{ij}	binary diffusion coefficient, cm ² /s
d	pipe diameter
H	Henry Law constant
k	reaction rate constant, 1/s
\dot{m}	diffusion mass flux, g/(cm ² s)
\dot{M}	mass flux, g/(cm ² s)
\dot{m}_{ir}	chemical transformation, g/(cm ³ s)

*Corresponding author, e-mail: tanselkoyun@sdu.edu.tr

\dot{n}_{ir}	reaction rate, mol/(cm ³ s)
P	pressure (atm)
R	pipe radius
R_i	specific gas constant, joule/(gK)
\bar{R}	universal gas constant, joule/(molK)
Re	Reynolds number
Sc	Schmidt number
S	area, cm ²
T	temperature, K
u	axial velocity, cm/s
v	radial velocity, cm/s
V	volume, cm ³
y	weight fraction (wt) (%)
x	axial coordinate

Greek symbols

α	loading (mol of CO ₂ /mol of amine)
μ	molecular weight, g/mol
σ_{ij}	Lennard-Jones parameters
$\Omega_{D,ij}$	Lennard-Jones parameters
ρ	density, g/cm ³
η	dynamic viscosity, g/(cm.s)
σ	weight factor
δ	film thickness, cm

Subscripts

0	value at the inlet
c	wall
D	diffusion
i	component
max	maximum
t	total

Superscripts

*	dimensionless
---	---------------

1. INTRODUCTION

Natural gas is one of the important fuels for heating, water heating, cooling and automotive fuels. Nowadays, it plays a critical role on energy supply. It is essential to purify the natural gas from its undesired gases although natural gas yielding a considerably reduced emission is the cleanest fuel among fossil fuels. Numerous researches have been conducted on solubility of carbon dioxide and hydrogen sulphur in alkanolamine aqueous solution.

There are some studies in literature on this subject. Among these, Jou et al. [1] assessed the solubility of CO₂ in a

solution containing 30% monoethanolamine (MEA) at eight different temperatures ranging from 0 to 150 °C and at CO₂ partial pressures ranging from 0.001 to 20.000 kPa. Similarly, Li and Shen [2] examined the solubility of hydrogen sulphur (H₂S) in N-methyldiethanolamine (MDEA) and monoethanolamine aqueous solutions at H₂S partial pressures ranging from 1 to 450 kPa and at temperatures 40, 60, 80 and 100 °C. The higher the H₂S partial pressure, the higher the loading capacity of H₂S in solution is observed. As for the temperature effect, the lower the temperature, the higher the H₂S loading is obtained. Faiz and Al-Marzouqi [3] studied the simultaneous absorption of CO₂ and H₂S from natural gas

using aqueous potassium carbonate solutions as the absorbent solvent while utilizing hollow fiber membrane contactors. Their results showed that lower concentrations of carbonate solutions resulted in higher absorption rates, while the presence of high bicarbonate concentrations in the solution was the main incentive for the enhanced reversible reactions and thus, lower absorption rates were achieved. Dong et al. [4] used a commercially available polyimide material Matrimid® as the benchmark polymer material in fabrication of hollow fibers for natural gas purification. High CO₂/CH₄ separation factors (ranging up to 67) are achieved which are among the highest reported for purely polymeric hollow fibers without post-treatments and exceeded the commonly reported bulk values of Matrimid®.

Yeh and Bai [5] used ammonia (NH₃) and monoethanolamine (MEA) solvents to clean the greenhouse gas emissions. Pagella and De Faveri [6] established a new process to reduce hydrogen sulphur (H₂S) from the gas streams. Lin and Shyu [7] examined the CO₂ absorption by amines in a packed column experimentally using the primary monoethanolamine (MEA) and third N-methyldiethanolamine (MDEA) in gas purifying. There have been also few theoretical studies to investigate the purification process in detail. Yigit [8] described a model of absorption process in the lithium bromide. Negny et al [9] developed a new numerical model to determine the amount of hydrodynamic effects on heat and mass transfer during the absorption for the laminar film on an alternating wall column. Hughes and Bott [10] have devised a model demonstrating the geometry of the fluids running

downwards inside and outside vertical tubes. Negny et al. [11] have examined numerically the heat and mass characteristics and the flow model for film stream on an alternating vertical column. Oztop and Akpınar [12] made a typical application to see the effects of velocities on mass transfer for convective drying of some products. They used finite volume method to predict time dependent moisture distribution in products at different inlet flow temperature. Results show good agreement between numerical and experimental values. Finally, the numerical technique and computer code are capable of modeling moisture distribution inside the rectangular moist products. Other related studies can be found in Refs. [17-19].

The main objective of this work is to understand the effects of axial and radial velocities on mass transfer during the purification of natural gas numerically. The above literature clearly shows that theoretical studies on purification process of natural gas absorbed by monoethanolamine (MEA) are limited and much less is known of how axial and radial velocity affects mass transfer in the purification process of natural gas. Thus, the study will help to scientific researchers and designers.

2. CONFIGURATION

The physical model is plotted in Fig. 1 with coordinates. In this figure, the natural gas flowing inside a vertical channel and monoethanolamine (MEA) flowing as a film along the inner wall of the channel is taken together for the purification process.

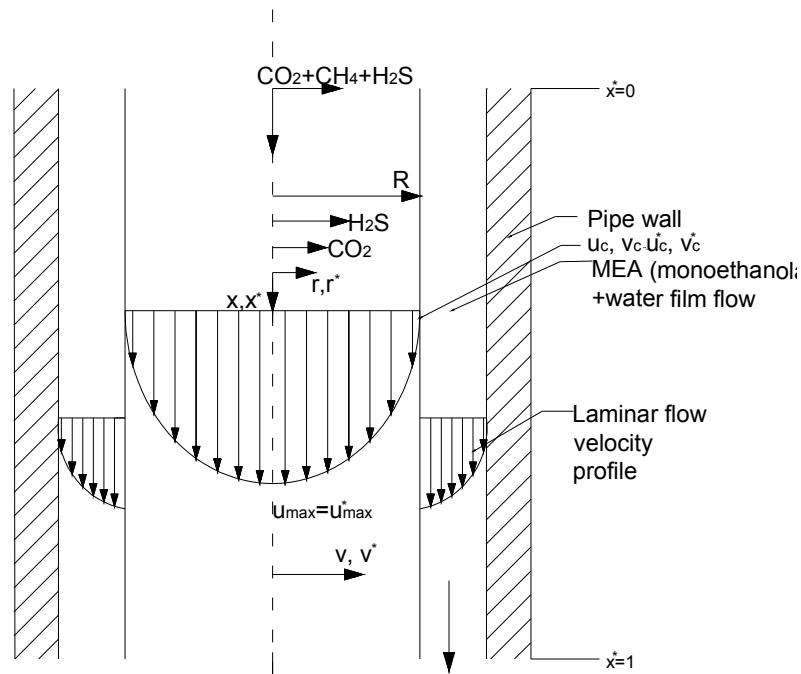


Fig. 1. Schematic representation of system.

3. EQUATIONS

Flow, continuity, mass transfer, ideal gas, gas absorption and film stream equations were used to analyze the purification process of natural gas. The equations of the system were expressed with dimensionless magnitudes comprising of Sherwood number (Sh), Schmidt number (Sc) and Damköhler number (Da) constituting the diffusion coefficients that determine the process. Polynary diffusion coefficients were calculated for continuous (barycentric) systems. The modified Stefan-Maxwell equation has been used as the basic equation when calculating the diffusion coefficients. After subsequently linearization of nonlinear terms in the partial derivative equation system obtained in a dimensionless manner, the solution has been achieved by Grams' finite differences method.

$$D_{ij,B} = [(y_j + y_k)\mu_i(\mu_k + y_k(\mu_j - \mu_k))\bar{D}_{ij}\bar{D}_{ik} + y_i\mu_j(\mu_k + y_k(\mu_i - \mu_k))\bar{D}_{ij}\bar{D}_{jk} + y_i y_k \mu_k (\mu_j - \mu_i)\bar{D}_{ik}\bar{D}_{jk}] / D \quad (3)$$

where coefficient D is defined as

$$D = y_i\mu_j\mu_k\bar{D}_{jk} + y_j\mu_i\mu_k\bar{D}_{ik} + y_k\mu_i\mu_j\bar{D}_{ij} \quad (4)$$

Dimensionless diffusion coefficients ($D_{AB,B}^*$, $D_{AC,B}^*$, $D_{BA,B}^*$, $D_{BC,B}^*$, $D_{CA,B}^*$, $D_{CB,B}^*$) are obtained considering polynary diffusion coefficients -

$D_{AB,B}$, $D_{AC,B}$, $D_{BA,B}$, $D_{BC,B}$, $D_{CA,B}$, and $D_{CB,B}$ and equations ($\mu_B^* = \mu_B / \mu_A$, $\mu_C^* = \mu_C / \mu_A$,

$D_{ij,B}^* = \frac{D_{ij,B}}{D_{AC}}$, $\bar{D}_{ij}^* = \frac{\bar{D}_{ij}}{D_{AC}}$). A sample formulation for

dimensionless polynary diffusion coefficient, $D_{AB,B}^*$, is given as follows:

$$D_{AB,B}^* = ((y_B + y_C)(\mu_C^* + y_C(\mu_B^* - \mu_C^*))\bar{D}_{AB}^* + y_A\mu_B^*(\mu_C^* + y_C(1 - \mu_C^*))\bar{D}_{AB}^*\bar{D}_{BC}^* + y_A y_C \mu_C^*(\mu_B^* - 1)\bar{D}_{BC}^*) / D' \quad (5)$$

Where \bar{D}_{AB}^* and \bar{D}_{BC}^* are dimensionless binary diffusion coefficients and D' is defined as

$$D' = y_A\mu_B^*\mu_C^*\bar{D}_{BC}^* + y_B\mu_C^* + y_C\mu_B^*\bar{D}_{AB}^* \quad (6)$$

3.1. Diffusion Theory (Ternary Diffusion)

The system was analyzed based on barycentric system, which is continuous and hydrodynamically active. In this case, the diffusion mass flux (\dot{m}_i) and mass flux (\dot{M}_i) are determined phenomenologically as follows:

$$\dot{m}_i = \rho \sum_{j=1}^N D_{ij,B} \frac{dy_j}{dr} \quad (1), \quad \dot{M}_i = \dot{m}_i + y_i \dot{M}_t \quad (2)$$

$j \neq i$

where $D_{ij,B}$ are polynary diffusion coefficients for barycentric systems ($I = A, B, C$). The general statement for ternary diffusion coefficients is [13]:

It is possible to calculate the dimensional binary diffusion coefficient for low-density (diluted) gases from the kinetic theory of gases. Based on the theory of Chapman-Enskog [14], binary diffusion coefficient is calculated as:

$$\bar{D}_{ij} = 1,8583 \cdot 10^{-27} \frac{\sqrt{T^3 \left(\frac{1}{\mu_i} + \frac{1}{\mu_j} \right)}}{P_1 \sigma_{ij}^2 \Omega_{\bar{D},ij}} \quad (7)$$

The binary diffusion coefficient depends proportionally on temperature and inversely proportional to molar masses and pressure. This means that \bar{D}_{ij} will increase with an increase in temperature, and decrease with an increase in molar masses and pressures. Both the dimensional and dimensionless binary diffusion coefficients calculated are presented in Table 1. The reaction rate definition for the i 'th component can be written based on the ideal gas equation as follows:

$$\dot{n}_{ir} = k_i c_i = k c x_i \quad (i = A, C \text{ components}) \quad (8)$$

In Eq.(8), x_i defines the ratio of the mole number of i component to total mole number and it is called as mole percentage. By substituting $P_i = \rho_i R_i T = H_i x_i$,

$R_i = \bar{R} / \mu_i$, $\rho_i = \rho y_i$ into the Eq.(8), chemical transformation (\dot{m}_{ir}) can be computed as;

$$\dot{m}_{ir} = \frac{k_i c \bar{R} T \rho y_i}{H_i} \quad (9)$$

If there is no mass transfer in the axial direction, the mass flow, \dot{M}_{ic} , on the wall is equal to the chemical transformation \dot{m}_{ir} . $\dot{M}_{BC} = 0$ for component B (CH₄) which is the passive gas on the wall. Thus, \dot{m}_{iD} can be rewritten as [13]:

$$\dot{m}_{iD} = \frac{k_i c \bar{R} T}{H_i} \delta \rho y_i - \rho y_i v_c \quad (10)$$

Where,

$$v_c = \frac{k_A c \bar{R} T \delta}{H_A} y_A + \frac{k_C c \bar{R} T \delta}{H_C} y_C \quad (11)$$

The dimensionless diffusion mass flux can be obtained using the following equations:

$$\dot{m}_{iD}^* = \dot{m}_{iD} \frac{R}{\rho_0 \bar{D}_{AC}} \quad (12)$$

$$v_c^* = \frac{2d}{D_{AC}} v \quad (13)$$

Then, the term \dot{m}_{iD}^* is obtained as

$$\dot{m}_{iD}^* = \frac{k_i c \bar{R} T}{\bar{D}_{AC} H_i} \delta \rho^* y_i - 0.25 \rho^* y_i v_c^* \quad (14)$$

Damköhler number (Da) which is an important parameter in the analysis of catalytic gas reactions defines the ratio of the reaction rate to diffusion rate. The first Damköhler number (Da₁) for “A” component and the second Damköhler number (Da₂) for “C” component are formulated as shown in Eq(15) and Eq(16) respectively;

$$Da_1 = \frac{k_A c \bar{R} T}{\bar{D}_{AC} H_A} \delta \quad (15)$$

$$Da_2 = \frac{k_C c \bar{R} T}{\bar{D}_{AC} H_C} \delta \quad (16)$$

The dimensionless parameter, v_c^* , can be calculated by

taking into account $v^* = 2v \frac{d}{D_{AC}}$,

$$v_c^* = 4Da_1 y_A + 4Da_2 y_C \quad (17)$$

the wall (namely film) interface mass transfer equations for A and C components have been shown as follows:

$$Da_1 y_A = -D_{AB,B}^* \left(\frac{\partial y_A}{\partial r^*} \right)_c + (D_{AC,B}^* - D_{AB,B}^*) \left(\frac{\partial y_C}{\partial r^*} \right)_c + \frac{1}{4} y_A v_c^* \quad (18)$$

$$Da_2 y_C = -D_{CB,B}^* \left(\frac{\partial y_C}{\partial r^*} \right)_c + (D_{CA,B}^* - D_{CB,B}^*) \left(\frac{\partial y_A}{\partial r^*} \right)_c + \frac{1}{4} y_C v_c^* \quad (19)$$

Similarly, if mass transfer occurs in the axial direction on the wall due to the interface velocity, the following equation can be expressed:

$$V \dot{m}_{ir} + \rho_i u_c S = (\dot{m}_{iD} + \rho_i v_c) S = \dot{M}_{ic} \quad (20)$$

Then, the dimensionless diffusion mass flux, \dot{m}_{iD}^* , can be re-derived as:

$$\dot{m}_{iD}^* = Da_i \rho^* y_i - \frac{1}{4} \rho^* y_i v_c^* + \frac{1}{2} \rho^* u_c^* y_i ReSc \quad (21)$$

With the combination of Eqs. (20) and (21) by replacing i with A and C components in Eq. (20), the radial velocity on the wall is obtained as [13]

$$v_c^* = 4Da_1 y_A + 4Da_2 y_C + 2 ReSc u_c^* \quad (22)$$

The axial velocity for the wall used in the equations above can be defined by Navier-Stokes equation subjected to Prandtl simplification as described by Kaufmann [15] including constant, laminar and compressible flow. Considering Navier-Stokes equations, the following equation can be defined as

$$\rho u \frac{\partial u}{\partial x} + \rho v \frac{\partial u}{\partial r} = -\frac{dP}{dx} + \eta_k \left[\frac{1}{r} \frac{\partial}{\partial r} \left(r \frac{\partial u}{\partial r} \right) \right] \quad (23)$$

Assuming fully developed flow conditions and $\rho v \frac{\partial u}{\partial r} = 0$

, integration of $\rho u \frac{\partial u}{\partial x}$ accounting boundary values ($r = 0$,

$u = u_{\max}$ and $r = R$, $u = u_c$) results in:

$$u = u_c + 2\bar{u}_0 \left(1 - \left(\frac{r}{R} \right)^2 \right) \quad (24)$$

$r^* = r/R$ and $u^* = u/\bar{u}_0$ if the equation is written in dimensionless form,

$$\text{At } r^* = 1, \quad u^* = u_c^*$$

$$\text{At } r^* = 0 \quad u_{\max}^* = u_c^* + 2$$

Above equations made dimensionless in the case with and without consideration of mass transfer due to the interface (wall) axial velocity, are solved separately with finite differences and adapted to the packaged program given by Gram [16]. The values calculated are shown in Table 2. These data and the equations obtained for $Re = 0$ and $Re = 2$ are adapted to the computer software and the results are illustrated in Figure 2 to 5. Where A, B and C stands for CO_2 , CH_4 and H_2S , respectively.

$$\mu_i^* = \frac{\mu_i}{\mu_A}; \text{ dimensionless molar mass for } i$$

$$\text{component, } \eta_i^* = \frac{\eta_i}{\eta_A}; \text{ dimensionless dynamic}$$

viscosity for i component.

The dynamic viscosity of mixture in the entrance, density in the entrance and molar mass of mixture are given as shown Eqs.(25-27) respectively;

$$\eta_{k0} = \frac{\sum y_{i0} \eta_i / \mu_i^{0.5}}{\sum y_{i0} / \mu_i^{0.5}} \quad (25)$$

$$\rho_0 = P_0 / R_0 T; \quad (26)$$

$$\mu_k = \frac{1}{\sum y_i / \mu_i} \quad (27)$$

4. NUMERICAL METHODS

Natural gas is absorbed by monoethanolamine (MEA) while running through a vertical pipe during the purification process. The equation system defining the isotherm pipe reactor consists of nonlinear parabolic differential equations. Due to the complex structure of the equation system defined above, it is impossible to achieve a solution with the classical method. Hence, the finite differences formulation is used in the solution of the equation system including partial derivatives. However, since this procedure can be applied to linear differential equations, the nonlinear terms in the equation system should be linearised and the result should be approached iteratively. Since the unknowns can be calculated pointwisely in the chosen numerical solution, the points have been determined with Δx^* and Δr^* axial and radial distances.

$$\Delta r_j^* = 0.1 / 2^j; j=1,2,3,\dots,7 \quad (28)$$

Small radial distances have been chosen near the pipe wall with respect to the stability of the problem for the numerical solution. The three terms in the obtained differential equations have been expressed as finite differences with the formulas below by Gram [16] as

$$U \frac{\partial u}{\partial x^*} = \left[(\sigma U'_{i,j+1} + (1-\sigma)U_{i,j}) (u_{i,j+1} - u_{i,j}) \right] / \Delta x^* \quad (29)$$

$$\frac{\partial u}{\partial r^*} = \left[\sigma (u_{i+1,j+1} - u_{i-1,j+1}) + (1-\sigma)(u_{i+1,j} - u_{i-1,j}) \right] / 2\Delta r^* \quad (30)$$

$$\frac{\partial}{\partial r} \left(F \frac{\partial u}{\partial r^*} \right) = \frac{1}{\Delta r^{*2}} \left\{ \sigma \left[F'_{i+\frac{1}{2},j+1} (u_{i+1,j+1} - u_{i,j+1}) - F_{i-\frac{1}{2},j+1} (u_{i,j+1} - u_{i-1,j+1}) \right] + \right.$$

$$+ (1 - \sigma) \left[F_{i+\frac{1}{2},j} (u_{i+1,j} - u_{i,j}) - F_{i-\frac{1}{2},j} (u_{i,j} - u_{i-1,j}) \right] \quad (31)$$

where U and F are symbols for variables. Subscripts i and j in Equations above are used for the variables in radial and axial directions. Forward direction for the first order derivative using 4 points is defined as

$$\frac{\partial y}{\partial h} = \frac{1}{6\Delta h} (-2y_4 + 9y_3 - 18y_2 + 11y_1) \quad (32)$$

Where, $h = r^*$. Concentration gradients on the wall can be computed as

$$\left(\frac{\partial y_i}{\partial r^*} \right)_{r^*=1} = \frac{1}{6\Delta r^*} (-2y_{i,38} + 9y_{i,39} - 18y_{i,40} + 11y_{i,41}) \quad (33)$$

The radial velocities are obtained by numerical integration using Trapezoidal rule and Simpson's rules.

$$v^* = -\frac{1}{r^* \rho^*} \int_0^{r^*} \frac{\partial}{\partial x^*} (r^* \rho^* u^*) dr^* \quad (34)$$

The equation systems obtained for u^* , y_A , and y_C are solved iteratively by Gauss elimination technique. With the iterative solution, the linearization magnitudes of U' and F' take the values computed at the previous iteration step. For values obtained at every iteration step, the relative error limit is assigned as

$$|(U - U')/U| \leq 10^{-4} \quad (35)$$

The implicit method is used in the numerical solution of the problem. The weight factor is taken $\sigma = 0.75$ in the computations due to the stability of the problem. The vertical tube inlet temperature is assumed to be 50°C for the calculations.

4. RESULTS AND DISCUSSION

A numerical study has been performed to analyze the purification of natural gas absorption via monoethanolamine (MEA). Effects of Damköhler number, Reynolds number and different reactant were tested.

Solubility of Carbon Dioxide (CO₂) in aqueous mixtures of monoethanolamine (MEA) with methyldiethanolamine (MDEA) has been measured at 40, 60, 80 and 100°C and at partial pressures of carbon dioxide between 1 and 200 kPa. The solubility of carbon dioxide (CO₂) in aqueous solutions is reported as functions of partial pressures of carbon dioxide at the temperatures studied. In this study, solubilities of CO₂ in 15.3 wt %MEA aqueous solution at 40 °C have been measured and the results are presented in Figure 2 .The solubility data obtained in this study are generally in good agreement with the data reported by other investigators in Figure 3. The higher the CO₂ partial pressures, the higher the CO₂ loading obtained in the alkanolamine aqueous solutions. Generally, the solubility of CO₂ with temperature; the higher temperature of the system, the lower the CO₂ solubility observed [14].

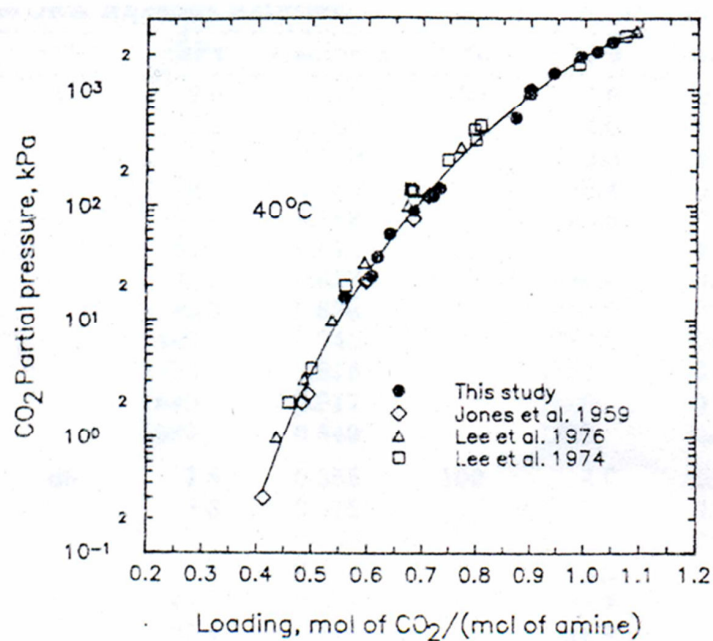


Fig. 2. Solubility of CO₂ in 15.3 wt % MEA aqueous solution at 40°C.

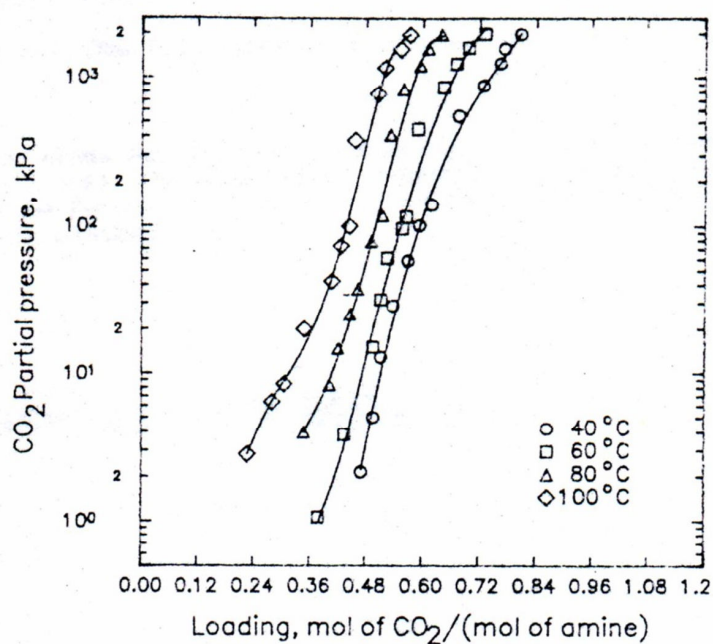


Fig. 3. Solubility of CO₂ in 30 wt % MEA aqueous solution at 40-100°C

Table 1. Dimensional and dimensionless binary diffusion coefficients for substance pairs.

Substance pairs	CO ₂ (A)-CH ₄ (B)	CH ₄ (B)-H ₂ S(C)	CO ₂ (A)-H ₂ S(C)
\overline{D}_{ij} (cm ² .s ⁻¹)	0.194	0.2	0.1373
\overline{D}_{ij}^*	1.413	1.4566	1

Table2. Physical properties of the components in the gas mixture.

Substance	y _i	μ _i (g/mol)	μ _i [*] $\mu_i^* = \frac{\mu_i}{\mu_A}$	η _i (g/cm.s)	η _i [*] $\eta_i^* = \frac{\eta_i}{\eta_A}$	ρ (g/cm ³)	Sc $Sc = \frac{\eta_{k0}}{\rho_0 \overline{D}_{AC}}$
CO ₂	0.2	44.01	1	16.211x10 ⁻⁵	-	-	-
CH ₄	0.7	16.04	0.3644	11.954x10 ⁻⁵	0.74	-	-
H ₂ S	0.1	34.09	0.7745	13.776x10 ⁻⁵	0.85	-	-
CO ₂ + H ₂ S (mixture)	CH ₄ + -	19.562 (μ _k)	-	12.6795x10 ⁻⁵ (η _{k0})	-	0.7381x10 ⁻³ (ρ ₀)	1.251

In this study, the results of numerical solution of purification of natural gas absorbed by monoethanolamine (MEA) are presented in Figure 4 through 5. The primary cause of molecular diffusion is the concentration gradients. Hence, the concentration area change must be known in order to examine the diffusion area. The change of the concentration profiles of A and C components at various X^{*} values are shown in Figure 4. The transformation

increased with the elevation of X^{*} and Γ^{*} values, but because of that Y_A and Y_C values decreased (Re = 0). The variation of the concentration profiles of A, C components at various X^{*} values as to the radial coordinate in Fig. 5 (a) and (b) drawn when Re exists in the obtained equations.

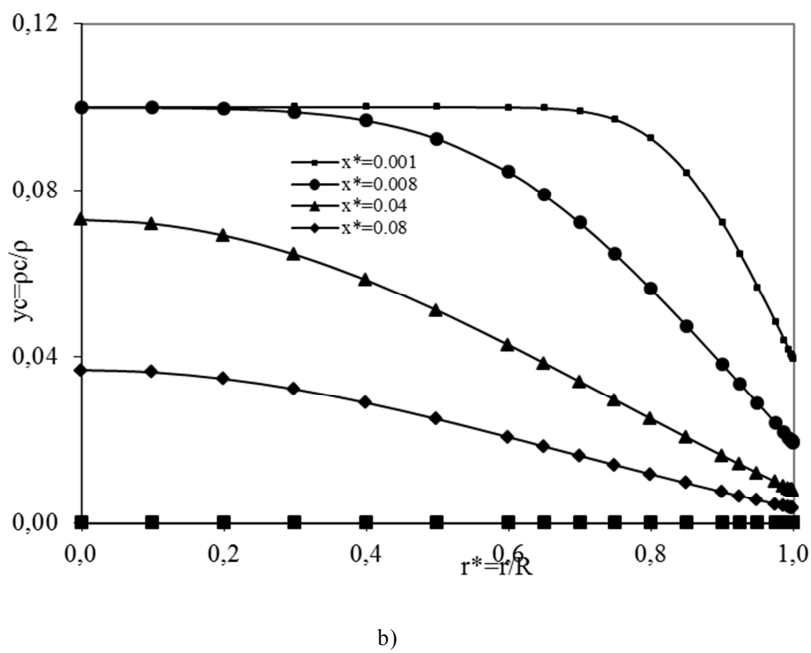
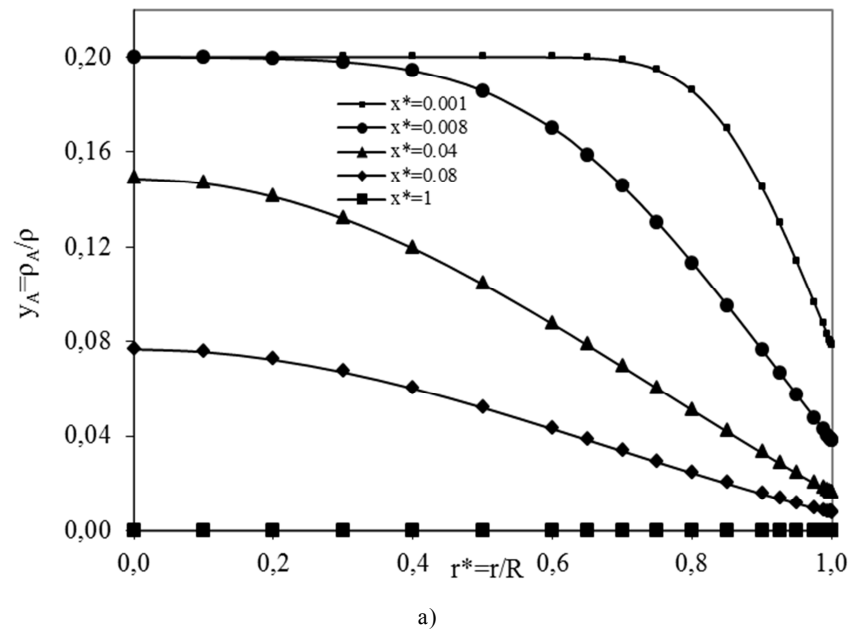
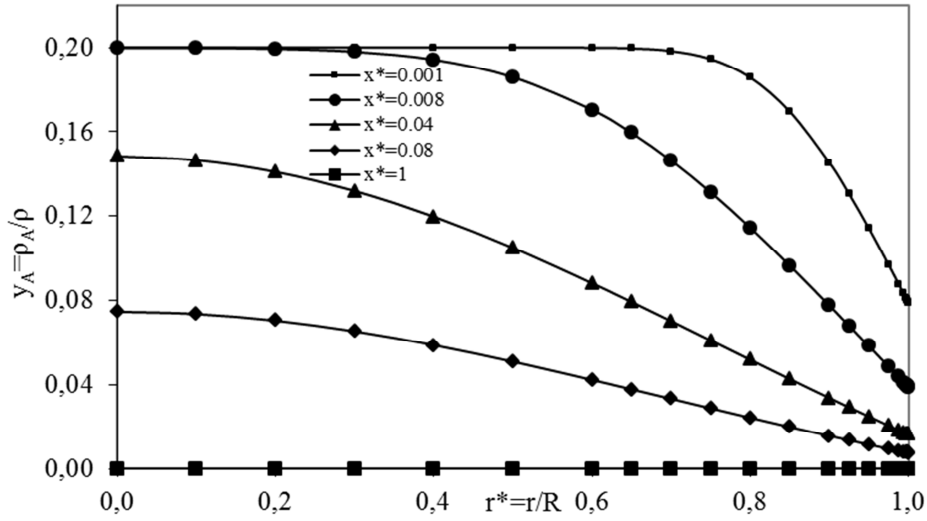
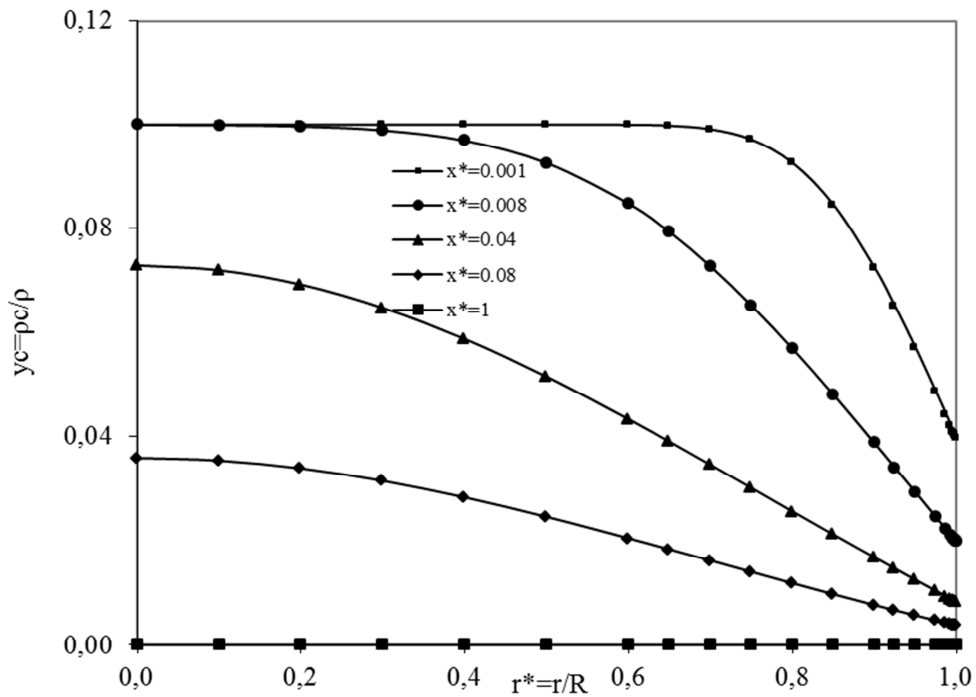


Fig. 4. The radial change of different reactants concentration at various values of dimensionless axial coordinate

$x^* = \frac{x}{d} \frac{1}{Re Sc}$, in the case of $Da = 15$ ($Re = 0$), a) A (CO_2), b) C (H_2S)



a)



b)

Fig. 5. The radial change of different reactants concentration at various values of dimensionless axial coordinate

$$x^* = \frac{x}{d} \frac{1}{Re Sc}, \text{ in the case of } Da = 15 \text{ (Re} = 2\text{), a) A (CO}_2\text{), b) C(H}_2\text{S)}$$

5. CONCLUSIONS

In this study, the process during the purification of natural gas is investigated. It is observed that the effect of interface axial flow velocity between natural gas and MEA can be neglected in mass transfer calculations. The effect of interface axial flow velocity is also negligible for $Re = 0$ and very small Re numbers, since the concentration change is resulted in A and C components as expected in the used Gram's packaged software. If the figures of both cases are compared, it can be seen that the correct results are obtained by taking the very low Reynolds number value into account in the interface axial direction. It is an important result that all calculations can be made for the case in $Re = 0$.

REFERENCES

- [1] Jou FY, Mather AE, Otto FD. "The Solubility of CO₂ in a 30 Mass Percent Monoethanolamine Solution", *The Canadian J. of Chemical Engineering*, 1995;73:140-147.
- [2] Li MH, Shen KP. "Solubility of Hydrogen Sulfide in Aqueous Mixtures of Monoethanolmine with N-Methyldiethanolamine", *Journal Chemical Engineering*, 1993;38:105-108.
- [3] Faiz R, Al-Marzouqi M. "Insights on natural gas purification: Simultaneous absorption of CO₂ and H₂S using membrane contactors", *Sep. Pur. Technology*, doi:10.1016/j.seppur.2010.11.005 (2010).
- [4] Dong G, Li H, Chen V. "Factors affect defect-free Matrimid® hollow fiber gas separation performance in natural gas purification", *J. Membrane Sci.*, 2010; 353:17-27.
- [5] Yeh AC, Bai H. "Comparison of Ammonia and Monoethanolamine Solvents to Reduce CO₂ Greenhouse Gas Emissions", *The Science of the Total Environment*, 1999;228:121-133.
- [6] Pagella C, De Faveri DM. H₂S "Gas Treatment by Iron Bioprocess", *Chem. Eng. Sci.* 2000; 55:2185-2194.
- [7] Lin SH, Shyu CT. "Performance Characteristics and Modeling of Carbondioxide Absorption by Amines in a Packed Column", *Waste Man.* 1999;19: 255-262.
- [8] Yigit A. A "Numerical Study of Heat and Mass Transfer in Falling Film Absorber", *Int. Com. Heat Mass Transfer* 1999;26:269-278.
- [9] Negny S, Meyer M, Prevost M. "Study of a Laminar Falling Film Flowing over a Wavy Wall Column.Part I –Numerical Investigation of the Flow Pattern and the Coupled Heat and Mass Transfer", *Int. J. Heat Mass Transfer* 2001;44:2137-2146.
- [10] Hughes DT, Bott TR. "Minimum Thickness of a Liquid Film Flowing Down a Vertical Tube", *Int. J. Heat Mass Transfer* 1998;41:253-260.
- [11] Negny N, Meyer M, Prevost M. "Enhancement of Absorbtion Efficiency for a Laminar Film Flow by Hydrodynamics Conditions Generated by a New Type of Column Wall", *Chemical Eng. J* 2001;83:7-13.
- [12] Oztop HF, Akpınar EK. "Numerical and Experimental Analysis of Moisture Transfer for Convective Drying of Some Products", *Int. Comm. in Heat Mass Transfer* 2008;35:169–177.
- [13] Koyun T. "Doğal Gazın Tasfiyesi Örneğinde Kütle Transferinin İncelenmesi", *Doktora Tezi*, Isparta, 2002. (In Turkish).
- [14] Uysal, BZ. "Kütle Transferi Esasları ve Uygulamaları", *Gazi Üniversitesi* 1996 (In Turkish).
- [15] Kaufmann W. "Technische Hydro und Aerodynamik", Berlin, *Springer-Verlag* 1963.
- [16] Gram, C. "Selected Numerical Methods", Copenhagen, 1962.
- [17] Shen KP, Li MH. "Solubility of Carbon Dioxide in Aqueous Mixtures of Monoethanolamine with Methyldiethanolamine", *J. Chem. Eng. Data* 1992;37:96-100.
- [18] Hillock AMW, Miller SJ, Koros WJ. "Crosslinked mixed matrix membranes for the purification of natural gas: Effects of sieve surface modification", *J. Membrane Sci.* 2008; 314:193-199.
- [19] Bergh J, Zhu W, Groen JC, Kapteijn F, Moulijn JA, Yajima K, et al., "Natural gas purification with a DDR zeolite membrane; permeation modelling with maxwell-stefan equations", *Studies in Surface Science Catalysis* 2007;170: 1021-1027.